Jurnal Ilmiah Teknik Elektro Komputer dan Informatika (JITEKI)
Vol. 8, No. 3, September 2022, pp. 354-366
ISSN: 2338-3070, DOI: 10.26555/jiteki.v8i3.24550

Trajectory Tracking and Collision Avoidance on Smart Wheel Chair

Munawar Agus Riyadi, Syuja Risqullah, Sumardi, Teguh Prakoso
Department of Electrical Engineering, Universitas Diponegoro, Jl. Prof. Sudharto, SH, Tembalang, Semarang 50275, Indonesia

ARTICLE INFO

Article history:

Received July 29, 2022
Revised October 04, 2021
Accepted October 05, 2021

Keywords:

Smart Wheelchair;
Kalman Filter;
IMU-9DOF;
Trajectory Tracking;
Collision Avoidance

ABSTRACT

There have been many developments of wheelchairs as mobility aids, including electric wheelchairs. Wheelchairs sometimes still require manual steering. Therefore, in this research, a smart wheelchair is developed that can move automatically to the destination position from a predetermined position with a trajectory tracking system. The system deploys the odometry method, orientation angle using the output of the IMU-9DOF sensor with Kalman filter, and collision avoidance to avoid collisions with obstacles in front of it. The use of the Kalman filter improves the angle output that is close to the reference. In the trajectory tracking test, the wheelchair can approach the given reference position with a maximum error of 20 cm for the x-axis and 2 cm for the y-axis. The wheelchair collision avoidance test has been able to avoid collisions, as it successfully detects an obstacle less than 40 cm and avoids the collision correspondingly.

Corresponding Author:

Munawar A. Riyadi, Department of Electrical Engineering, Universitas Diponegoro, Jl. Prof. Sudarto, SH, Tembalang, Semarang 50275, Indonesia
Email: munawar@elektro.undip.ac.id

1. INTRODUCTION

It is estimated that about 15% of the population in the world lives with disabilities, according to World Report on Disability [1][2]. Disabilities can be found due to physical disability, injury, or caused diseases on motoric muscles or nerves [3]. In turn, disabilities may limit mobility for many people to do their activities or to move freely.

For people who have a certain degree of mobility limitations, a wheelchair is of great help. Manual wheelchairs require the use of the patient's hands or assistance from others for the movement. For people who have limited hand movement or patients with partial tetraplegia, sclerosis, parkinsonism, and stroke due to paralysis of some limbs, which are still unable to operate them themselves, they must be assisted by others. Several researchers have tried to develop a better version of the wheelchair. Some wheelchairs have been developed with voice commands as motion commands [4][5] or by the use of head movement to direct the wheelchair's motion [6]-[9]. Another innovation proposed the use of eye blink as a command source, thus making it easier for users or patients to move without using their hands [10][11] or by using electrooculography (EOG) [12]-[15]. Another approach is by using brainwaves as a source of command [15]-[18]. These improvements make the users move with minimum assistance and be more independent. Others developed intelligent wheelchairs designed to avoid obstacles in front of them [19][20]. The collision avoidance feature helps the user to prevent crashing into a wall or hitting other objects automatically. This is a great improvement, as the users lack the response time to make an abrupt change in controlling the wheelchair.

However, some approaches may limit the usage in the long term, manifested in mental breakdown due to the long, intense brain concentration or as the frequent use of eye blinks for command leads to fatigue in the eye muscles and may result in motion errors [18]. Similar cases can also be affected by intervention or noise, as is the case of the wheelchair with voice commands in a very noisy environment. On the other hand, for domestic or hospital use, the path of movement for a disabled person with a wheelchair is usually predictable

[21]-[25]. For instance, he/she usually needs to trip from one room to other parts of the building several times daily. This routine can be taken as a predetermined path that can be put into the wheelchair's smart system. With a simpler command, the routine can be handled easier and involve less effort in the command. Sahin et al. [21] proposed a path-tracking wheelchair. Unfortunately, it is only for the wall following, not for predetermined targets.

Therefore, in this paper, we present a novel approach to making it easier for wheelchair users to move through a track that is routinely passed by users. A wheelchair is developed using the trajectory tracking system that can move automatically from one position to another with a predetermined orientation angle by measuring the distance and angle that the wheelchair must travel. In addition, another improvement is also presented in the form of a collision-avoidance feature to enhance the safety of the user.

2. METHOD

2.1. Mechanical Hardware Design

As the base of the wheelchair, we use a manual wheelchair that meets the SNI standard (Indonesian National Standard) and then equip it with additional motors and controllers. Each left and right wheel is coupled with a DC motor using chain-connected gear. The gear ratio between the DC motor and wheel is 1:2.5. The PG 45 DC motor is coupled to a large gear on the wheel shaft with a small gear on the DC motor shaft using a chain to reduce the load on the DC motor when in use. The hardware design is shown in Fig. 1. Additional details of the wheelchair design can be found in this reference [26].

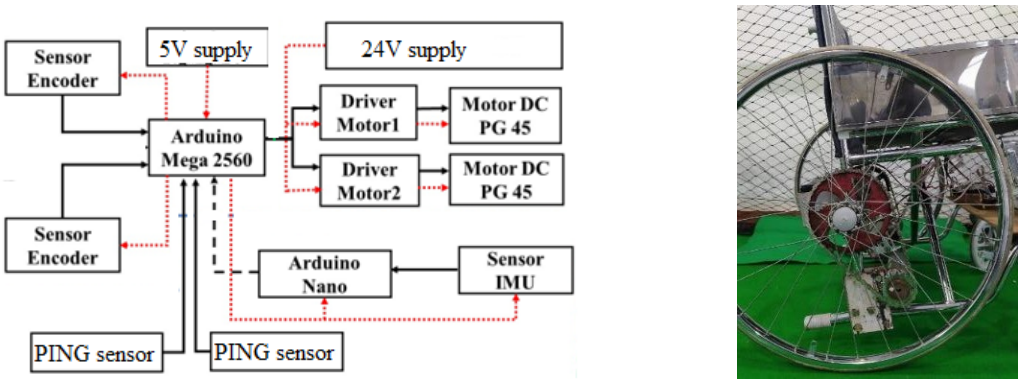

(a) (b)

Fig. 1. (a) Block diagram of Hardware design, (b) wheel driver mechanism

2.2. Odometry

Odometry is a data processing method that comes from the actuator movement to get an estimate of changes in position from time to time. To get odometry data, an encoder sensor is needed. The position relative to the initial position can be estimated using Odometry [27]-[30]. Each number of pulses issued by the rotary encoder sensor will be converted into a distance unit, which then obtains information on the relative position of the wheelchair.

The number of pulses per unit rotation of the wheel is calculated using the following equations:

$$K_{wheel} = 2\pi R \tag{1}$$

$$Pulse = \frac{R_{enc}}{K_{wheel}} \tag{2}$$

Where is K_{wheel} the circumference of the wheel, R is the radius of the wheel, and R_{enc} is the resolution of the encoder (number of pulses in full revolutions).

In the differential drive system, there are two separate actuators, each connected to a wheel, namely the left and right wheels. The distance traveled by each wheel is the left and right distance (D_L and D_R, respectively), and the pulse detected by odometry for the left and right wheel is $Pulse_L$ and $Pulse_R$, respectively. The distance between the two wheels is L, then by knowing the actual pulse per centimeter of each wheel ($Pulse_{CM}$), the actual distance (D_{act}) and the orientation angle (OA_{rad}) are determined as follows:

$$D_L = \frac{Pulse_L}{Pulse_{CM}} \tag{3}$$

$$D_R = \frac{Pulse_R}{Pulse_{CM}} \tag{4}$$

$$D_{act} = \frac{D_L + D_R}{2} \tag{5}$$

$$\theta_{rad} = \frac{-D_L + D_R}{L} \tag{6}$$

The orientation angle is still in radian units, which can be changed to degrees (θ_{deg}), later introduced as the heading:

$$\theta_{deg} = \frac{180}{\pi}\theta_{rad} \tag{7}$$

After knowing the actual distance and orientation angle, the position at coordinate X (Pos_x) and coordinate Y (Pos_y) can be determined as [29]

$$Pos_x = V_s \cos\theta_{deg} \tag{8}$$

$$Pos_y = V_s \sin\theta_{deg} \tag{9}$$

$$\omega = 2\pi f = 2\pi \frac{encoder}{R_{enc}} \tag{10}$$

$$V_s = (\omega_R + \omega_L)\frac{R}{2} \tag{11}$$

Where ω is the angular speed, f is the rotation frequency, R is the radius of the wheel, ω_R is the right angular speed (rad/s), ω_L is the left angular speed (rad/s), and V_s is wheelchair speed. The calculation of the actual distance value will be reset back to 0 when it is finished in one cycle of movement.

2.3. Trajectory Tracking

Trajectory tracking is provided so that the wheelchair can move to another position automatically by providing a trajectory in the form of a Cartesian plan that the wheelchair must follow [22], [31]. The wheelchair moves by following the trajectory by providing a value for the destination position from the odometry calculation. Equations (8) and Equations (9) are used to determine the position of the wheelchair on the Cartesian axis in cm. The shape of the area used in the Cartesian coordinate system can be seen in Fig. 2 for a sample of domestic movement between the bedroom, toilet (WC), dining room, and living room. The trajectory may vary for different house layouts, but in principle, the common track is represented here, with the option of a right-and-left turn.

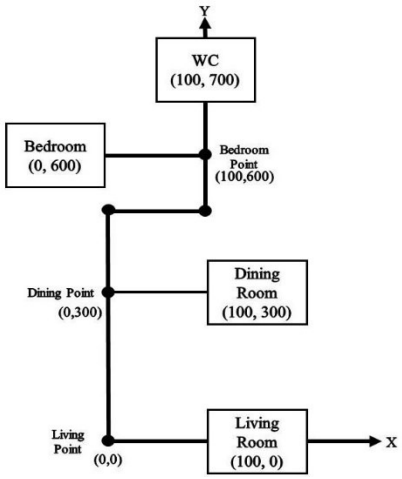

Fig. 2. Coordinate plan of domestic trajectory

2.4. IMU Angle 9 DOF

The wheelchair orientation angle is obtained from the IMU 9 DOF sensor by combining data from three sensors, namely the accelerometer, gyroscope, and magnetometer, using the sensor fusion method. The equation used to obtain IMU 9 DOF sensor data is as follows [32].

Accelerometer equation is

$$Roll: \tan\theta = \frac{a_z}{a_y} \tag{12}$$

$$Pitch: \tan\phi = \frac{a_x}{\sqrt{a_y^2 + a_z^2}} \tag{13}$$

Gyroscope equation is

$$Roll: \theta = \omega_\theta \, \Delta t \tag{14}$$

$$Pitch: \phi = \omega_\phi \, \Delta t \tag{15}$$

$$Yaw: \psi = \omega_\psi \, \Delta t \tag{16}$$

Magnetometer is

$$Yaw: \psi = \tan^{-1}\frac{m_y}{m_x} \tag{17}$$

Where a_x, a_y and a_z are the data of the x-, y- and z-axis of the accelerometer, respectively, while ω_θ , ω_ϕ and ω_ψ are the angular velocity of the gyroscope roll, pitch, and yaw. In addition, m_x, m_y and m_z represent the data of the x-axis, y-axis, and z-axis of the magnetometer.

The next step is to combine data from the accelerometer and magnetometer to get the heading in yaw (Ψ) angle value, with the following equation [32] as

$$M_x = m_x \cos\phi + m_z \sin\phi \tag{18}$$

$$M_y = m_x \sin\theta \sin\phi + m_y \cos\theta - m_z \sin\theta \cos\phi \tag{19}$$

$$\psi = \tan^{-1}\frac{M_x}{M_y} \tag{20}$$

2.5. Kalman Filter

Kalman filter is used to reduce the noise emitted by the sensor before the sensor output is sent as input to a control system [33][34]. Noisy data may make the system have the wrong response. The Kalman filter does not need data to be stored, and the data is reprocessed for every measurement. Kalman filter is divided into two main parts, namely time update and measurement update. Time update is also called the prediction process, namely by getting the current state estimate from the previous time estimation state. Meanwhile, the measurement update is also known as the correction process, which is getting an accurate estimation state by using the current measurement information to improve predictions [35]. The equations contained in the prediction and correction process are as follows [36].

Time Update equations are

$$Estimation: \hat{x}_{k|k-1} = A\hat{x}_{k|k-1} + BU_{k-1} \tag{21}$$

$$Error\ covariant: P_{k|k-1} = AP\hat{x}_{k|k-1}A^T + Q_k \tag{22}$$

Measurement Update equations are

$$K\ Gain: k_k = P_{k|k-1}H^T + BU_{k-1} \tag{23}$$

$$Estimation: \hat{x}_{k|k} = \hat{x}_{k|k-1} + K_k(Z_k - H\hat{x}_{k|k-1}) \tag{24}$$

$$Error\ covariant: P_{k|k} = (I - K_k H)P_{k|k-1} \quad (25)$$

Where A is the state transition matrix, B is the input control matrix, Q is the covariance of the noise process, H is the observation matrix, R is the noise covariance, P is the covariance estimation matrix, K is the Kalman gain, and I is the identity matrix. Kalman filter is implemented for the noise filtering process of the IMU (Inertial Measurement Unit) sensor output data before the data is processed by the microcontroller.

2.6. Collison avoidance

Collision Avoidance is used so that wheelchairs can avoid accidents from collisions with objects in front of them, either wall, door, person, or obstacles. This system works by changing the speed of the wheelchair based on the distance between the wheelchair and the object in front of it [19][37].

In this collision avoidance system, there is only one decision. Namely, the wheelchair will stop if one of the ultrasonic sensors detects a distance less than a given threshold with an object or something in front of it. In the collision avoidance system, this study uses two ultrasonic PING sensors (on each front side, right, and left) to obtain distance value information. The PING ultrasonic sensors emit ultrasonic waves with a frequency of 40 kHz into the air for 200µs, where the ultrasonic waves will propagate in the air at a speed of 344.42 m/s or takes 29.034µs for each cm [38][39].

To determine the distance, the PING sensor transmits and receives the ultrasound signal. By measuring half the time to travel of pulse width (forth and back), the distance can be calculated using the following equation [38]:

$$distance = \frac{1}{2}\frac{pulsewidth}{29.034} \quad (26)$$

3. RESULTS AND DISCUSSION

3.1. Encoder Turnover Pulse Test

The PG45 DC motor has an encoder reading value in one rotation from the factory or also called a tick, of 537.6. By using two gears coupled to a chain, the wheelchair has a reduction of 2.5. Thus, the wheel has an encoder or tick reading. The value of 537.6 times 2.5 is 1344. Using the factory default tick still has an error. The following is the rotation wheel pulse test data in Table 1.

The test is carried out by comparing several wheels tick values with the mileage set to 100 cm, then compared with the actual measured distance using a ruler. From Table 1, it can be seen that the encoder reading value in one wheel rotation from the factory default 1344 calculation has an error of 6.5 cm, and the closest to the reference value of 100 cm is pulse 1250, with the smallest error of 0.3 cm.

Table 1. Encoder Rotation Pulse Data

No	Encoder Value (tick)	Read Distance (Centimeter)	Measured Distance (Centimeter)	Error (Centimeter)
1	1344	100	106.5	6.5
2	1300	100	105.3	5.3
3	1290	100	104.9	4.9
4	1275	100	102.3	2.3
5	1250	100	100.3	0.3

3.2. PING sensor testing

PING ultrasonic sensor testing is done by detecting the distance of a solid object which is likened to an obstacle in front of a wheelchair. The results of the distance measurement read by the sensor and measured by the meter can be seen in Table 2 and Table 3. In Table 2, the right distance sensor test has the largest error of 0.9% at 40 cm distance measurement, while the smallest is 0.03% at 60 cm measurement with an overall average error of 0.44%, so it does not have much effect on the system. In Table 3, the test of the left proximity sensor has the largest error of 0.9% at a distance measurement of 20 cm, while the smallest is 0.08% at a distance measurement of 80 cm with an overall average error of 0.49%. The average error of the proximity sensor is not too large, so it doesn't have much effect on the system.

3.3. Kalman Filter Test and IMU Orientation Angle

The Kalman filter test is carried out by comparing the value of reading coarse data from the sensor, data after being filtered by complement, and data after being filtered with a Kalman filter, with angle values of 0°, 45°, and 90°. The filter results can be seen in Fig. 3 – Fig. 5.

Table 2. Right PING Sensor Test Data

No	Read Distance (Centimeter)	Measured Distance (Centimeter)	Error (Centimeter)	Error (%)
1	20.1	20	0.1	0.49
2	40.4	40	0.4	0.9
3	60.02	60	0.02	0.03
4	80.45	80	0.45	0.5
5	100.3	100	0.3	0.29
Average			0.254	0.44

Table 3. Left PING Sensor Test Data

No	Read Distance (Centimeter)	Measured Distance (Centimeter)	Error (Centimeter)	Error (%)
1	20.2	20	0.2	0.9
2	40.31	40	0.31	0.7
3	60.34	60	0.34	0.5
4	80.07	80	0.07	0.08
5	100.3	100	0.38	0.3
Average				0.26

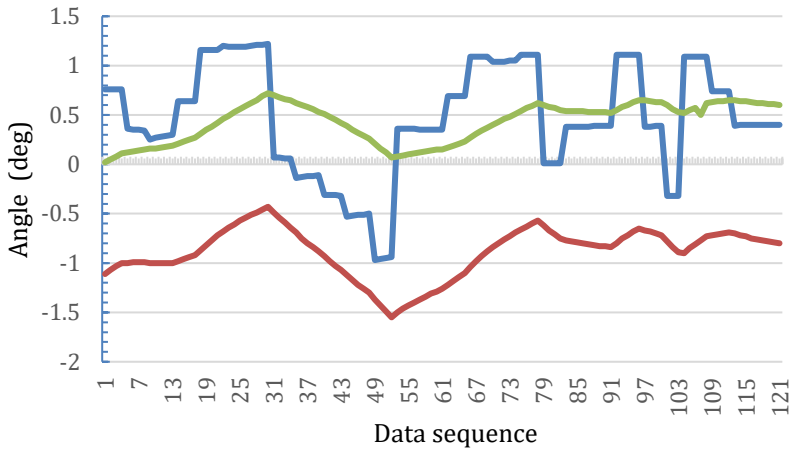

Fig. 3. Kalman Filter Comparison Results for 0°angle (blue line: yaw raw data, red: complement, green: after Kalman filter)

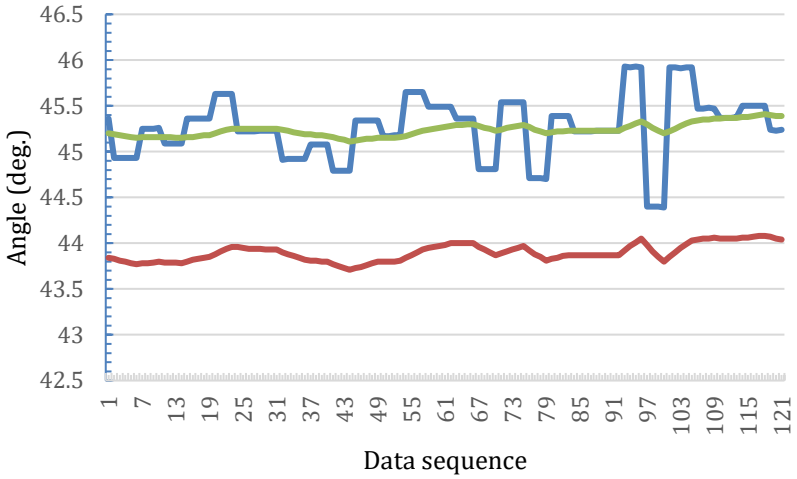

Fig. 4. Kalman Filter Comparison Results for 45°angle (blue line: raw yaw data, red: complement, green: after Kalman filter)

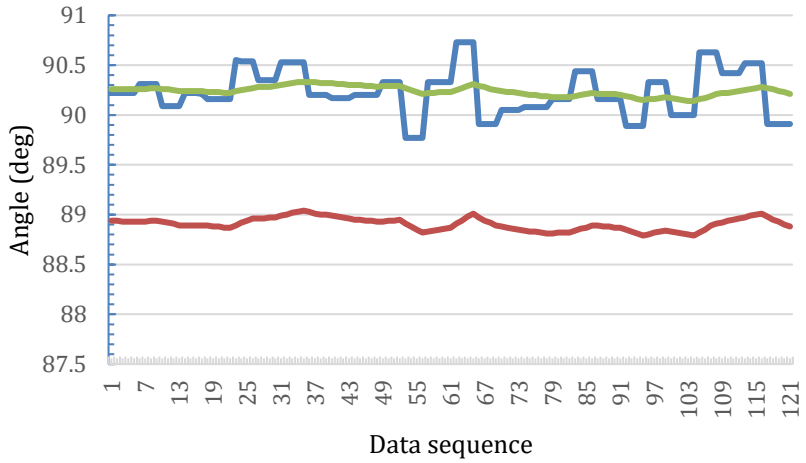

Fig. 5. Kalman Filter Comparison Results for 90°angle (blue line: yaw raw data, red: complement, green: after Kalman filter)

From Fig. 3 - Fig. 5, it can be seen that the angle value that has been filtered with the Kalman filter has improved so that it does not oscillate too much when compared to the coarse data. Meanwhile, the angle data filtered by the complement filter has a data value that is not too oscillating but has a slightly different value from the coarse sensor output data. The results of measuring the angle of the wheelchair orientation using the IMU 9 DOF sensor, which is read with and measured by an arc, are shown in Table 4.

Table 4. Arc Measured Angle Value Data and Sensor Read

No	Arc (degrees)	Sensor (degrees)	Error (degrees)	Error (%)
1	45	45.48	0.48	1.05
2	90	90.85	0.85	0.93
3	135	135.27	0.27	0.19
4	180	180.26	0.26	0.14
Average			0.465	0.57

Table 4 shows that the angle measured by the arc and read by the sensor has an average error equal to 0.465 or 0.57%. The biggest error occurred in the measurement of the angle equal to 90°, with the value read by the sensor equal to 90.85°. This is because, at the time of testing, the IMU sensor experienced a shift, which should be at the exact point it should be.

3.4. Zero Point Trajectory Tracking Testing to Living Room

Testing the displacement from the zero point or guest point to the living room is carried out by moving two steps toward the target. In this test, the wheelchair will move according to the given coordinates without calculating the wheelchair heading angle and the resultant distance by providing a coordinate setpoint of (100, 0) cm. In the first step, the wheelchair will turn right is 90° then proceed to move on the x-axis is 100 cm. the following is a graph of the results of the wheelchair movement test in Fig. 6. It shows the final position of the wheelchair is at (110: -7) cm. The wheelchair can approach the predetermined destination position, namely (100:0) cm. So, the error value about the x-axis is equal to 10 cm, and the y-axis is equal to -7 cm. The error occurs due to the oscillation of motion in the wheelchair, which is another effect of using the PID control to reach the setpoint and synchronize between the wheels and the continued motion due to the nature of the DC motor, which does not lock in the final position [6].

3.5. Zero Point Trajectory Tracking Testing to the Dining Room

Testing the displacement from the zero point or the guest point to the dining room is carried out by moving two steps toward the target. In this test, the wheelchair will move according to the given coordinates without calculating the wheelchair heading angle and the resultant distance by providing a setpoint coordinate of (100,300) cm. In the first step, the wheelchair will move straight on the y-axis as far as 300 cm, followed by moving on the x-axis for a distance of 100 cm. the following is a graph of the results of the wheelchair movement test in Fig. 7. It shows the final position of the wheelchair at (100,99:286). The wheelchair moves on the y-axis and then moves on the x-axis. When moving on the y-axis, the wheelchair appears to move

slightly to the left by - 12 cm for the x-axis so that it is offset by about 12 cm to the left, and the wheelchair only reaches a distance of 300 cm in the first step. Meanwhile, when moving on the x-axis, the wheelchair also experiences an offset of 0.99 cm, so the final value on the x-axis is 100.99 cm. The final result on the y-axis with a position of 286 cm occurs because when the wheelchair turns, the DC motor does not lock its position, so there is a follow-up movement that occurs [6]. Error events like this can occur due to several factors, including the different performance of the two actuators even though they are given the same input, the floor slope factor, and the oscillation of the wheelchair movement, which is another effect of using PID control to reach the setpoint.

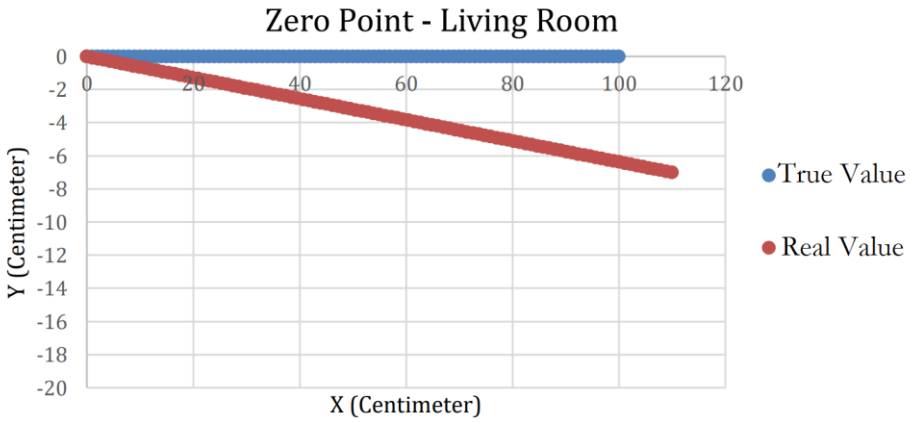

Fig. 6. Results of the Move from Point Zero to the Living Room (not to scale)

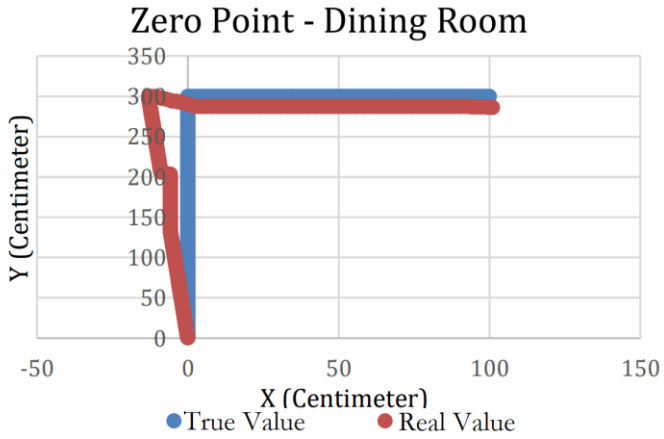

Fig. 7. Results of the Move from Point Zero to the Dining Room

3.6. Zero Point Trajectory Tracking Testing to the Bedroom

Testing the displacement from the zero point or the guest point to the bedroom is carried out by moving two steps toward the target. In this test, the wheelchair will move according to the given coordinates without calculating the wheelchair heading angle because the orientation angle is obtained from the IMU sensor and the resultant distance by providing a coordinate setpoint of (0, 600) cm, the first step the wheelchair will move straight for 500 cm on the y-axis then proceed by moving on the x-axis as far as 100 cm to the right against the x-axis, then 100 cm up against the y-axis, and ending with a straight left 100 cm about the x-axis, here is the graph of the results wheelchair movement test in Fig. 8. It shows the final position of the wheelchair at coordinates (-4:603) cm. When moving on the y-axis, the wheelchair seems to move slightly to the left, with a final result of -21 cm for the x-axis. This is because the floor in that position is uneven, and the wheelchair only reaches a distance of 500 cm on the x-axis. y first step. Meanwhile, when the second step moves to the right for the x-axis, the wheelchair also experiences an offset of -20 cm. This happens because of the offset that occurred earlier so that by 80 cm, the wheelchair has turned left. In the second step, the position of the wheelchair on the y-axis is also offset. This is because when the wheelchair turns, the DC motor does not lock its position [6].

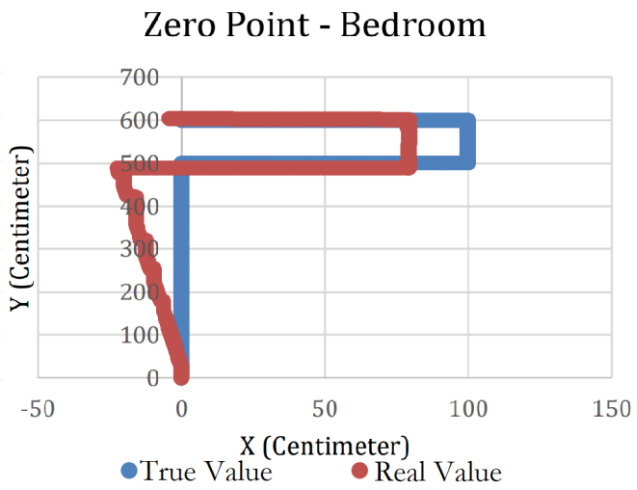

Fig. 8. The Result of Moving from Point Zero to the Bedroom

3.7. Zero Point Trajectory Tracking Testing to Toilet (WC)

Testing the movement from the zero point or guest point to the WC is carried out by moving three steps to get to the target. In this test, the wheelchair will move according to the given coordinates without calculating the wheelchair heading angle because the orientation angle is obtained from the IMU sensor and the resultant distance by providing a coordinate setpoint of (100, 700) cm, the first step the wheelchair will move straight for 500 cm on the y-axis, the second step moves on the x-axis as far as 100 cm to the right, then proceeds to move straight on the y-axis for 200 cm. The following is a graph of the results of the wheelchair movement test in Fig. 9.

Fig. 9 shows the final position of the wheelchair at the coordinates (80:702). The wheelchair moves on the y-axis then moves on the x-axis then moves straight again on the y-axis. When the first step moves on the y-axis, the chair appears to have an error by turning left by 4 cm to the left against the x-axis or -4 cm and has an offset of 2 cm from the y-axis so that the final value of the first step is in the coordinates (-4:502). In the second step, the wheelchair looks quite stable, there is no error in the y-axis, but there is an error in the distance that should be covered, which is 100 cm, while the distance taken is 84 cm with an offset of -4 cm in the first step so that the second step has a coordinate value end (80:502).

In the third step, the wheelchair looks quite stable and does not experience too many errors on the x-axis and y-axis, with the final coordinate value (80: 702). Error occurrences like this can occur due to several factors, including the different performance of the two actuators even though they are given the same input or the oscillation of movement in the wheelchair, which is another effect of using PID control to reach the setpoint.

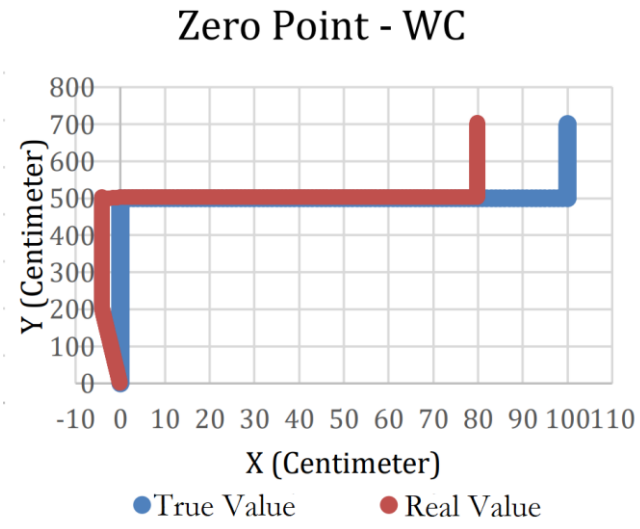

Fig. 9. Result of Transfer from Zero Point to WC

3.8. Collision Avoidance Testing in Straight Path

The test is carried out by placing an obstacle in front of the wheelchair while it is moving in a straight path. The following is a graph of the results of testing the proximity sensor in Fig. 10. It shows the distance sensor detects an obstacle with a distance of less than 40 cm and the wheelchair stops. This is indicated by the constant value of the distance traveled by the wheelchair, seen at stops 1 and 2. In the detection of the first obstacle, the wheelchair stops with a distance of constant wheelchair mileage at 140 cm, and on detection of obstacles, both wheelchairs stop with constant wheelchair mileage at 292 cm.

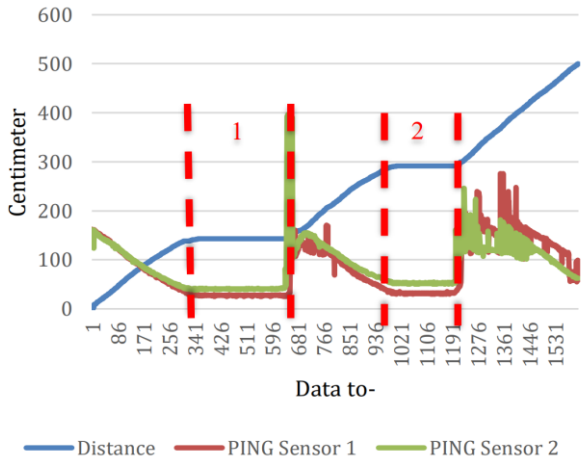

Fig. 10. PING Sensor Detection Results Manual Mode

3.9. Collision Avoidance Testing on Trajectory Tracking

The test was carried out by placing an obstacle in front of the wheelchair while it was moving in trajectory-tracking mode from the zero point to the toilet. The following is a graph of the results of the proximity sensor test when in manual mode in Fig. 11. The result shows that when the distance sensor detects an obstacle with a distance of less than 40 cm, the wheelchair stops. This is indicated by the constant value of the distance traveled by the wheelchair, seen at stops 1 and 2. In the detection of the first obstacle, the wheelchair stops with a distance of constant wheelchair travel at 240 cm, and on detection of obstacles, both wheelchairs stop with constant wheelchair mileage at 654 cm. When the obstacle is no longer detected by the sensor, the wheelchair continues trajectory tracking to completion.

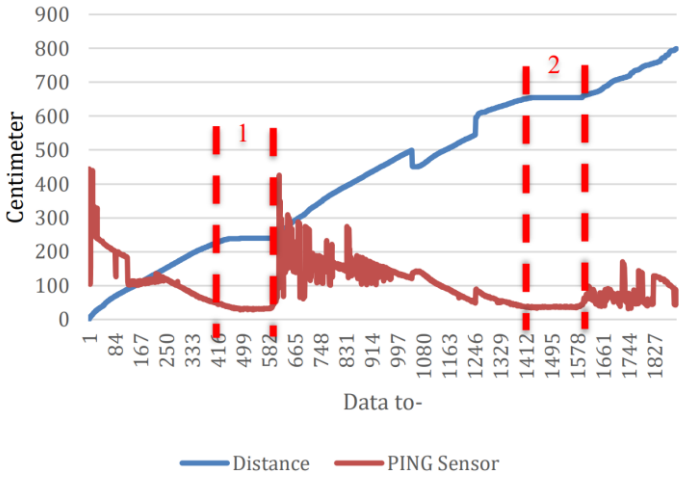

Fig. 11. PING Sensor Detection Results Trajectory Tracking Mode

3.10. Discussion

The overall test shows that the developed wheelchair can perform the trajectory tracking mode. The test has been conducted for the track with a straight path and with a right/left turn for different scenarios. The trajectory error and final location error did happen in all tests. The actual position that is closest to the reference

position is at the reference position (-4;603) cm, which should be at (0;600) cm, with an error on the x-axis equal to 4 cm and 3 cm on the y-axis. At the same time, the most distance is at the reference position (80;702) cm, which should be at (100;700) cm, with an error on the x-axis equal to 20 cm and 2 cm on the y-axis. The error occurs due to motion oscillation which is another effect of using PID control to keep the two wheels in sync, which is also evident in other research [40]. The error in the final position is also affected by the slip, which may happen for multi-stage motor-wheel coupling with a chain. The slip thus accumulated in odometry error, as was the case in [41]. On the other hand, surface slip may add to the equation, as in [42]. As a comparison, the path-tracking of an electric wheelchair in [43] also resulted in about a 5cm error for 10-s movement. The error value is not affected by the value of the reference position and the order of movement of the destination. In addition, there is an error in the final destination of all tests due to a follow-up motion due to the nature of the DC motor, which does not lock the final position. Therefore, the result indicates the capability of the proposed approach to follow the path.

In the collision avoidance test with the ultrasonic sensor, when the sensor detects an obstacle less than 40 cm, the wheelchair shows the capability to stop and will continue its movement until it is finished if it doesn't detect it anymore. A different approach was taken by [19] by adding a bumper. However, the short space offered (±20 mm) is too risky and has very small room for error. Several tests also show that the halt is not time-dependent but obstacle-distance-dependent. Therefore, the proposed collision avoidance has worked well as designed.

4. CONCLUSION

In this study, the smart wheelchair has been successfully developed with the capability of trajectory tracking and also features collision avoidance. The design of smart wheelchairs is based on using an odometry system and distance information from two ultrasonic sensors. The wheelchair performance in all tests shows the prospective result. The path-trajectory test with the simulated domestic route shows that the wheelchair is capable of following various tracks, either straight or with turns, with acceptable accuracy. Moreover, with the additional capability of collision avoidance which enables the wheelchair to stop within 40 cm of obstacles, the wheelchair can add to safety for the user during its movement and avoid the crash to door, walls, people, or other objects. With this improvement offered (trajectory tracking and collision avoidance), the wheelchair has the potential to be applied for further usage

Acknowledgments

This work is supported by Universitas Diponegoro under RPP Grant 2021-2022.

REFERENCES

[1] M. Rembis and H. P. Djaya, “Gender, Disability, and Access to Health Care in Indonesia: Perspectives from Global Disability Studies,” *in Transforming Global Health, Cham: Springer International Publishing*, pp. 97–111, 2020, https://doi.org/10.1007/978-3-030-32112-3_7.

[2] V. Ningrum, W.-C. Wang, H.-E. Liao, A. Bakar, and Y.-H. Shih, "A special needs dentistry study of institutionalized individuals with intellectual disability in West Sumatra Indonesia," *Scientific Reports*, vol. 10, no. 1, pp. 1-8, 2020, https://doi.org/10.1038/s41598-019-56865-2

[3] M. A. M. Berger, M. van Nieuwenhuizen, M. van der Ent, M. van der Zande, “Development of a new wheelchair for wheelchair basketball players in the Netherlands,” *Procedia Engineering*, vol. 34, 2, pp. 331-336, 2012, https://doi.org/10.1016/j.proeng.2012.04.057.

[4] S. Sohail and M. S. Saleem, "Sabertooth Based Smart Electric Wheelchair with Advanced Features," *Pakistan Journal of Scientific Research*, vol. 1, no. 1, pp. 14-17, 2021, https://doi.org/10.57041/pjosr.v1i1.4.

[5] M. Nishimori, T. Saitoh, and R. Konishi, “Voice controlled intelligent wheelchair,” *Proc. SICE Annu. Conf.*, no. October 2007, pp. 336–340, 2007, https://doi.org/10.1109/SICE.2007.4421003.

[6] M. Mudassir and A. Mujahid, “Modeling and Fabrication of Smart Robotic Wheelchair Instructed by Head Gesture,” *Indones. J. Electr. Eng. Informatics*, vol. 9, no. 3, pp. 633–646, 2021, https://doi.org/10.52549/.v9i3.2892.

[7] P. Dey, Md Mehedi Hasan, Srijon Mostofa, and Ariful Islam Rana. "Smart Wheelchair Integrating Head Gesture Navigation," *In 2019 International Conference on Robotics, Electrical and Signal Processing Techniques (ICREST),* pp. 329-334, 2019, https://doi.org/10.1109/ICREST.2019.8644322.

[8] R. Solea, A. Margarit, D. Cernega, A. Serbencu, "Head Movement Control of Powered Wheelchair," *23rd International Conference on System Theory, Control and Computing (ICSTCC)*, pp. 632-637, 2019, https://doi.org/10.1109/ICSTCC.2019.8885844.

[9] R. Abid, F. Hamden, M. A. Matmati, and N. Derbel. "Fuzzy Control of an Intelligent Electric Wheelchair Using an EMOTIV EPOC Headset," *In Advanced Systems for Biomedical Applications, Springer, Cham*, pp. 261-286, 2021, https://doi.org/10.1007/978-3-030-71221-1_12.

[10] H. G. M. T. Yashoda, A. M. S. Piumal, P. G. S. P. Polgahapitiya, M. M. M. Mubeen, M. A. V. J. Muthugala, and A. G. B. P. Jayasekara, "Design and Development of a Smart Wheelchair with Multiple Control Interfaces," *2018*

Moratuwa Engineering Research Conference (MERCon), pp. 324-329, 2018, https://doi.org/10.1109/MERCon.2018.8421945.
[11] W. C. Francis, C. Umayal, and G. Kanimozhi, "Brain-Computer Interfacing for Wheelchair Control by Detecting Voluntary Eye Blinks," *Indones. J. Electr. Eng. Informatics,* vol. 9, no. 2, May 2021, https://doi.org/10.52549/ijeei.v9i2.2749.
[12] Q. Huang et al., "An EOG-based Wheelchair Robotic Arm System for Assisting Patients with Severe Spinal Cord *Injuries," J. Neural Eng.,* vol. 16, no. 2, 2019, https://doi.org/10.1088/1741-2552/aafc88.
[13] Y. Li, S. He, Q. Huang, Z. Gu, and Z. L. Yu, "A EOG-based Switch and its Application for "Start/Stop" Control of a Wheelchair," *Neurocomputing*, vol. 275, pp. 1350-1357, 2018, https://doi.org/10.1016/j.neucom.2017.09.085.
[14] Q. Huang, Y. Chen, Z. Zhang, S. He, R. Zhang, J. Liu, Y. Zhang, M. Shao, and Y. Li, "An EOG-based Wheelchair Robotic Arm System for Assisting Patients with Severe Spinal Cord Injuries*," Journal of Neural Engineering*, vol. 16, no. 2, p. 026021, 2019, https://doi.org/10.1088/1741-2552/aafc88.
[15] Q. Huang, Z. Zhang, T. Yu, S. He, and Y. Li, "An EEG-/EOG-based Hybrid Brain-Computer Interface: Application on Controlling an Integrated Wheelchair Robotic Arm System," *Frontiers In Neuroscience*, vol. 13, p. 1243, 2019, https://doi.org/10.3389/fnins.2019.01243.
[16] S. K. Swee, L. Z. You, and K. T. Kiang, "Brainwave Controlled Electrical Wheelchair," *MATEC Web Conf.*, vol. 54, pp. 3–6, 2016, https://doi.org/10.1051/matecconf/20165403005.
[17] A. Palumbo, V. Gramigna, B. Calabrese, and N. Ielpo, "Motor-imagery EEG-based BCIs in Wheelchair Movement and Control: A Systematic Literature Review," *Sensors*, vol. 21, no. 18, p. 6285. 2021, https://doi.org/10.3390/s21186285.
[18] A. Dev, M. A. Rahman, and N. Mamun, "Design of an EEG-Based Brain Controlled Wheelchair for Quadriplegic Patients," *3rd Int. Conf. Converg. Technol*, pp. 1-5, July 2019, https://doi.org/10.1109/I2CT.2018.8529751.
[19] S. Ishida and H. Miyamoto, "Collision-Detecting Device for Omnidirectional Electric Wheelchair," *ISRN Robot.,* vol. 2013, pp. 1–8, 2013, https://doi.org/10.5402/2013/672826.
[20] A. K. M. B. Haque, S. Shurid, A. T. Juha, M. S. Sadique, and A. S. M. Asaduzzaman, "A Novel Design of Gesture and Voice Controlled Solar-Powered Smart Wheel Chair with Obstacle Detection*," In 2020 IEEE International Conference on Informatics, IoT, and Enabling Technologies (ICIoT), IEEE*, pp. 23-28, 2020, https://doi.org/10.1109/ICIoT48696.2020.9089652.
[21] H. İ. Şahin and A. R. Kavsaoğlu, "Autonomously Controlled Intelligent Wheelchair System for Indoor Areas," *3rd International Congress on Human-Computer Interaction, Optimization and Robotic Applications (HORA)*, pp. 1-6, 2021, https://doi.org/10.1109/HORA52670.2021.9461335.
[22] F. P. de Paiva, E. Cardozo, and E. Rohmer, "A Path Tracking Control Algorithm for Smart Wheelchairs," 2020 *International Symposium on Medical Robotics (ISMR),* pp. 76-82, 2020, https://doi.org/10.1109/ISMR48331.2020.9312939.
[23] D. Tak, A. Jain, P. S. Savnani and D. Akash Mecwan, "Path Tracing in Holonomic Drive System with Reduced Overshoot using Rotary Encoders," *7th International Conference on Signal Processing and Integrated Networks (SPIN), Noida, India,* pp. 343-348, 2020, https://doi.org/10.1109/SPIN48934.2020.9071196.
[24] T. A. Bahtiyar, F. Ardilla, B. S. Marta and D. Pramadihanto, "Effectiveness of bicycle path planning method and pure pursuit method on omni-directional mobile robot," *International Conference on Control, Electronics, Renewable Energy and Communications (ICCEREC)*, pp. 91-97, 2015, https://doi.org/10.1109/ICCEREC.2015.7337061.
[25] Y. Jung, Y. Kim, W. H. Lee, M. S. Bang, Y. Kim, and S. Kim, "Path Planning Algorithm for an Autonomous Electric Wheelchair in Hospitals," *in IEEE Access,* vol. 8, pp. 208199-208213, 2020, https://doi.org/10.1109/ACCESS.2020.3038452.
[26] M. I. Andreansyah, S. Sumardi, T. Prakoso, and M. A. Riyadi, "Pengaruh Berat Pengguna Terhadap Kontrol Kecepatan Motor DC Menggunakan Kontroler PID Untuk Pergerakan Kursi Roda Pintar," *J. Teknol. dan Sist. Komput.,* vol. 20, April 2022, https://doi.org/10.14710/jtsiskom.2022.14358.
[27] J.-x. Wang and X. Cui, "Rotary Encoder Based Self-Positioning Method for Mobile Robot," *5th International Conference on Information Science and Control Engineering (ICISCE)*, pp. 500-504, 2018, https://doi.org/10.1109/ICISCE.2018.00111.
[28] M. Enkhbold, D. Nanzadragchaa, and M. Bayarpurev, "Coordinate Estimation Scheme for Differential Mobile Robots Using Rotary Encoder," *IEEE Transportation Electrification Conference and Expo, Asia-Pacific (ITEC Asia-Pacific)*, pp. 1-5, 2019, https://doi.org/10.1109/ITEC-AP.2019.8903816.
[29] E. Papadopoulos and M. Misailidis, "On Differential Drive Robot Odometry with Application to Path Planning," *in European Control Conference (ECC)*, pp. 5492–5499, 2007, https://doi.org/10.23919/ECC.2007.7068785.
[30] Z. T. Romadon, H. Oktavianto, I. K. Wibowo, B. Sena Bayu Dewantara, E. A. Nurrohmah, and R. Adryantoro Priambudi, "Pose Estimation on Soccer Robot using Data Fusion from Encoders, Inertial Sensor, and Image Data," *International Electronics Symposium (IES)*, pp. 454-459, 2019, https://doi.org/10.1109/ELECSYM.2019.8901578.
[31] S. Saat, A. R. M. Kamil, M. Z. M. Tumari and A. S. R. A. Subki, "Development of an autonomous robot for inspection system," *IEEE 14th International Colloquium on Signal Processing & Its Applications (CSPA)*, pp. 272-276, 2018, https://doi.org/10.1109/CSPA.2018.8368725.
[32] L. Tran, "Data Fusion with 9 Degrees of Freedom Inertial Measurement Unit To Determine Object's Orientation," Senior project, EE Dept, California Polytechnic State University, 2017, https://digitalcommons.calpoly.edu/eesp/400/.

[33] V. Sangale and A. Shendre, "Localization of a Mobile Autonomous Robot Using Extended Kalman Filter," Third *International Conference on Advances in Computing and Communications*, pp. 274-277, 2013, https://doi.org/10.1109/ICACC.2013.59.
[34] Y. Choudhary, N. Malhotra, P. K. Sahoo, and S. Kamal, "Data-Driven Modeling of a Track-based Stair-Climbing Wheelchair," *IEEE/ASME International Conference on Advanced Intelligent Mechatronics (AIM)*, pp. 1000-1005, 2021, https://doi.org/10.1109/AIM46487.2021.9517494.
[35] D. Feng, C. Wang, C. He, Y. Zhuang, and X. -G. Xia, "Kalman-Filter-Based Integration of IMU and UWB for High-Accuracy Indoor Positioning and Navigation," *in IEEE Internet of Things Journal*, vol. 7, no. 4, pp. 3133-3146, April 2020, http://dx.doi.org/10.1109/JIOT.2020.2965115.
[36] M. Al-Gabalawy, N. S. Hosny, J. A. Dawson, and A. I. Omar, "State of charge estimation of a Li-ion battery based on extended Kalman filtering and sensor bias," *International Journal of Energy Research*, vol. 45, no. 5, pp. 6708-6726, 2021, https://doi.org/10.1002/er.6265.
[37] P. S. Savnani, H. S. Sisodia, D. Tak and A. Mecwan, "Modelling, Design and Control of a Four wheel Holonomic Drive," *7th International Conference on Signal Processing and Integrated Networks (SPIN)*, pp. 879-884, 2020, https://doi.org/10.1109/SPIN48934.2020.9070971.
[38] S. Suherman, R. A. Putra and M. Pinem, "Ultrasonic Sensor Assessment for Obstacle Avoidance in Quadcopter-based Drone System," *3rd International Conference on Mechanical, Electronics, Computer, and Industrial Technology (MECnIT),* pp. 50-53, 2020, https://doi.org/10.1109/MECnIT48290.2020.9166607.
[39] P. A. Darwito, M. Raditya, H. Sa'diyah, A. Cikadiarta and W. Aditya, "Comparative Study of Burst And Beams Types Ultrasonic Sensor For Distance Measurements," *2019 International Seminar on Intelligent Technology and Its Applications (ISITIA)*, 2019, pp. 46-51, https://doi.org/10.1109/ISITIA.2019.8937133.
[40] N. Hasanah, A. H. Alasiry, and B. Sumantri, "Two Wheels Line Following Balancing Robot Control using Fuzzy Logic and PID on Sloping Surface," *International Electronics Symposium on Engineering Technology and Applications (IES-ETA)*, pp. 210-215, 2018, https://doi.org/10.1109/ELECSYM.2018.8615483.
[41] D. M. W. Boey, "Odometry Error Reduction in Wheelchair Using More Than One Sensor.," PhD dissertation, UTAR, 2019, http://eprints.utar.edu.my/id/eprint/3457.
[42] O. Chuy, E. G. Collins, C. Ordonez, J. Candiotti, H. Wang, and R. Cooper, "Slip mitigation control for an Electric Powered Wheelchair," *Proc. - IEEE Int. Conf. Robot. Autom.,* no. May, pp. 333–338, 2014, https://doi.org/10.1109/ICRA.2014.6906632.
[43] K. K. Ahn, J. I. Yoon, and D. K. Khoa, "A Study on the Path-Tracking of Electric Wheelchair Robot*," J. Korean Soc. Precision Eng.*, vol. 28, no. 11, pp. 1265–1271, 2011, https://koreascience.kr/article/JAKO201106654856568.page.